Enhancing Angle Estimation for Off-Boresight Targets Using Biomimetic Antenna Arrays

Patrik Grüner, Son Nguyen, Tobias Chaloun, Christian Waldschmidt
Institute of Microwave Engineering, Ulm University, Ulm, Germany
patrik.gruener@uni-ulm.de

***Abstract* — Biomimetic Antenna Arrays (BMAAs) are able to enhance the angle estimation of miniaturized radar sensors by mimicking the hearing system of a fly. This technique has significant advantages over conventional approaches when only limited space is available. While recent works show the enhancement for targets in the vicinity of the boresight direction only, this work presents a more generalized design methodology to enhance the angle estimation for off-boresight targets. Radar measurements of a realized BMAA have been conducted and show a significant increase in angle estimation capability compared to a conventional antenna array at a target angle of 20 degrees.**

***Keywords* — Biomimetic Antenna Array, Direction-of-arrival estimation, Radar Systems.**

I. Introduction

Biomimetic Antenna Arrays (BMAAs) are antenna systems which allow angle estimation despite a small separation of its antenna elements. They increase the phase difference between the radiating elements by using a coupling inspired by the hearing system of the fly *Ormia ochracea*. This fly achieves an angle estimation accuracy of 2° with an acoustical aperture of $\lambda/20$ only [1].

Up to now, BMAAs were only used to increase the angle estimation capability for targets in the vicinity of the boresight direction of the antenna [2], [3], [4]. For targets under higher incidence angles, the angle estimation still degrades because the phase difference curve flattens out towards higher angles. It is shown in this paper that by extending the current BMAA theory the point of maximum sensitivity can be symmetrically shifted out of the boresight region to higher angles. A design criterion is derived and a BMAA with increased angle estimation capability at 20° was fabricated and measured.

II. Biomimetic Antenna Arrays

This sections briefly summarizes the terms and metrics used to describe the Biomimetic Antenna Array (BMAA). The basic principle of a two-element BMAA with antenna element spacing d is shown in Fig. 1. An incident plane wave under an angle θ from the boresight direction leads to a phase progression of $\phi_{\text{in}} = kd\sin\theta$ at the antenna terminals with $k = 2\pi/\lambda$ the wave number in free space. A special coupling between the antennas which mimics the auditory system of the fly *Ormia ochracea* is then applied by the BMAA. The phase progression ϕ_{out} after this biomimetic coupling is hereby significantly increased compared to the uncoupled case (c.f. Fig. 2 for the case η=5 and ξ=0) This comes at the cost of a loss in output power level [3].

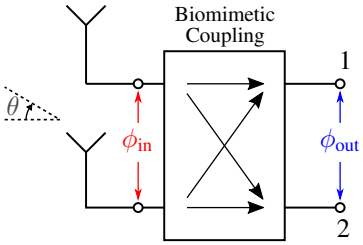

Fig. 1. BMAA principle [3].

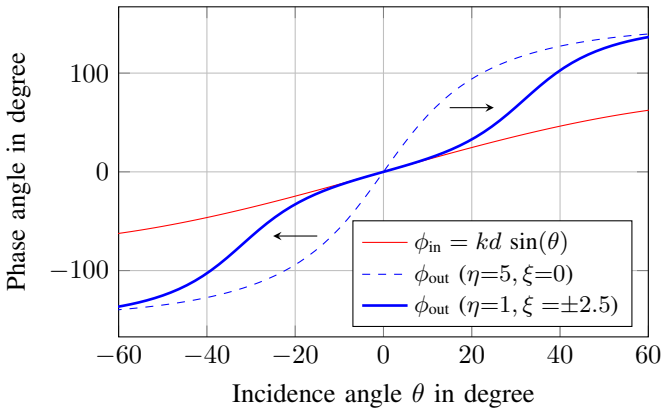

Fig. 2. Output phase difference for boresight and non-boresight case.

On the system level, the BMAA can be described by the two parameters phase gain η and normalized output power L_{out} [3], [5]. The phase gain, or phase enhancement factor, is defined by the ratio of the slopes of the respective phase progression curves at the terminals of a BMAA (ϕ_{out}) and a regular antenna array (ϕ_{in}) in boresight direction:

$$\eta = \frac{\left.\frac{\mathrm{d}\phi_{\text{out}}}{\mathrm{d}\theta}\right|_{\theta=0}}{\left.\frac{\mathrm{d}\phi_{\text{in}}}{\mathrm{d}\theta}\right|_{\theta=0}} . \tag{1}$$

The decrease in output power level is quantified by the dimensionless quantity L_{out}:

$$L_{\text{out}} = \frac{P_{\text{out,BMAA}}}{P_{\text{out,reg. Array}}} . \tag{2}$$

This quantity indicates the power level at the output of the BMAA normalized to the power level of a regular antenna array using the same radiating elements with similar spacing d but without biomimetic coupling. This value is always less than or equal to 1.

III. BMAAs for Off-Boresight Operation

Starting from the definitions in Section II, the necessary adjustments for the off-boresight operation of BMAAs are described in this section. All investigations are based on the electrical model of the BMAA introduced in [2], [5]. According to [2], the output phase difference for a BMAA with a physical antenna element spacing d calculates to

$$\phi_{\text{out}}(\theta) = \arctan\left(\frac{2\alpha\eta}{1-\alpha^2(\eta^2+\xi^2)}\right) , \tag{3}$$

with $\alpha{=}\phi_{\text{in}}/2{=}kd\sin\theta/2$, θ the incidence angle, η the phase gain in boresight direction defined in (1) and a parameter ξ. This parameter ξ was not yet studied in detail. Its impact on the course of the phase difference can be seen in Fig. 2. For $\xi = 0$, the ϕ_{out} curve has its maximum slope at the boresight direction. This is the well known behaviour of current BMAAs. Setting $\xi \neq 0$ the point of maximum slope of the ϕ_{out} curve can be shifted symmetrically to higher angles of incidence. In the following, a procedure will be shown how to achieve an output phase difference curve which has its steepest slope at a desired incidence angle θ_{ob}.

At first, a generalized phase enhancement factor has to be defined which is valid for all incidence angles θ, not only for the boresight region. It is defined as in (1) without the constraint $\theta{=}0$, i.e. the quotient of the derivatives of $\phi_{\text{out}}(\theta)$ and $\phi_{\text{in}}(\theta)$ for every incidence angle θ. This results in the generalized phase enhancement factor η_{ob}:

$$\eta_{\text{ob}}(\theta) = \frac{\eta(1+(\eta^2+\xi^2)\tan^2(\alpha))\sec^2(\alpha)}{1+(\eta^2+\xi^2)^2\tan^4(\alpha)+2(\eta^2-\xi^2)\tan^2(\alpha)} . \tag{4}$$

It can be directly verified that for boresight directions ($\theta{=}\alpha{=}0$) the generalized phase gain η_{ob} converts into the previously defined phase gain η. The point of maximum slope shall now be placed at higher incidence angles. Therefore it is assumed in the following that the phase gain η in boresight direction is 1.

To find the angle θ_{ob} where the phase enhancement factor is highest, (4) is differentiated with respect to α and set to zero. The resulting equation is then rearranged with respect to ξ. For $\eta{=}1$, $0{<}\alpha_{\text{ob}}{<}\frac{\pi}{2}$ the (real) value of ξ is then :

$$\xi = \pm\frac{1}{\sin\alpha_{\text{ob}}}\sqrt{-2+\cos(2\alpha_{\text{ob}})+\frac{\sqrt{7+\cos(4\alpha_{\text{ob}})}}{\sqrt{2}}} . \tag{5}$$

Equation (5) gives a direct relation between the desired angle α_{ob} ($\propto \theta_{\text{ob}}$) of maximum phase gain and the necessary value for ξ. For high angles θ_{ob}, the parameter ξ is tending towards 0 while it is going towards infinity for small desired angles θ_{ob}.

Although (5) allows to set the maximum slope of the ϕ_{out} curve to the desired angle, its slope steepness cannot be directly controlled as it is shown in Fig. 3. Here, for a given antenna, the coupling networks were designed so that the maximum slopes of the output phase difference curve is at $\theta_{\text{ob}}{=}30°$ and $\theta_{\text{ob}}{=}50°$, respectively, leading to a phase gain of $\eta_{\text{ob}}{\approx}21$ and

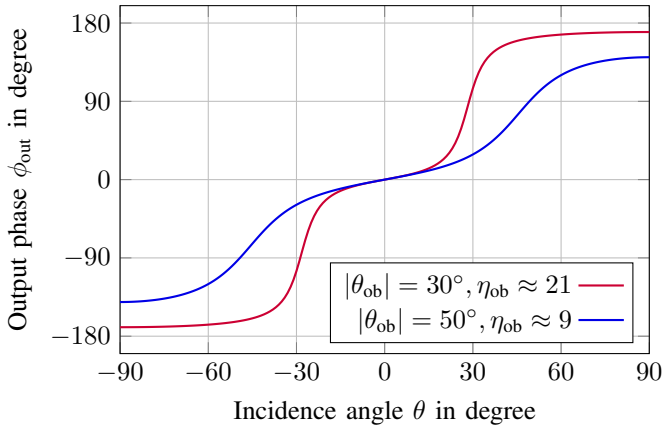

Fig. 3. Output phase difference for a given antenna array with different values of ξ and $\eta = 1$.

$\eta_{\text{ob}}{\approx}9$. For a given antenna and $\eta{=}1$, the slope of the ϕ_{out} curve therefore gets more and more flat for higher angles θ_{ob} leading to a smaller phase enhancement factor η_{ob}.

By using the generalized phase enhancement factor η_{ob} and the angle dependant output power level L_{out}, the quality criterion found in [6] is still valid and needs to be fulfilled for an enhanced angle estimation under the desired angle θ_{ob}:

$$\eta_{\text{ob}}(\theta_{\text{ob}})\sqrt{L_{\text{out}}(\theta_{\text{ob}})} > 1 . \tag{6}$$

IV. Fabricated BMAA

Based on the findings described in the previous chapters, a biomimetic antenna array for the frequency range of 20 GHz was fabricated. As the current theory was not modified, the only parts that need to be modified, compared to current BMAAs, are the coupling network parameters. The BMAA is designed to have its maximum slope of ϕ_{out} at $\theta_{\text{ob}} = \pm 22°$. The antenna design is based on the BMAA presented in [3] and consists of two aperture coupled patch antennas separated by a distance of $d = \lambda/5$. The coupling network consists of the susceptances B_1 and B_2 as well as a conductance G_L. The corresponding layout is shown in Fig. 5. Compared to [3], the straight stubs were replaced by radial stubs which can be chosen smaller and which are more broadband. The radial stubs with length r_o act as shunt capacitors realizing B_1, the thin connecting line with length l_{conL} and width w_{conL} acts as an inductance realizing B_2. The power is coupled out by an $\lambda/4$-transformer with length l_{l4} and width w_{l4} assuring the correct G_L. The equivalent lumped element parameters B_1, B_2 and G_L were determined by solving the two equations for η and ξ from [5] with the constraint of achieving the maximum possible L_{out}:

$$\eta = \frac{(G^2-G_{12}^2)+ab}{(G-G_{12})^2+a^2} \stackrel{!}{=} 1, \tag{7}$$

$$\xi_{\text{ob}} = \frac{G(b-a)-G_{12}(b+a)}{(G-G_{12})^2+a^2} \stackrel{!}{=} \pm 3.9 . \tag{8}$$

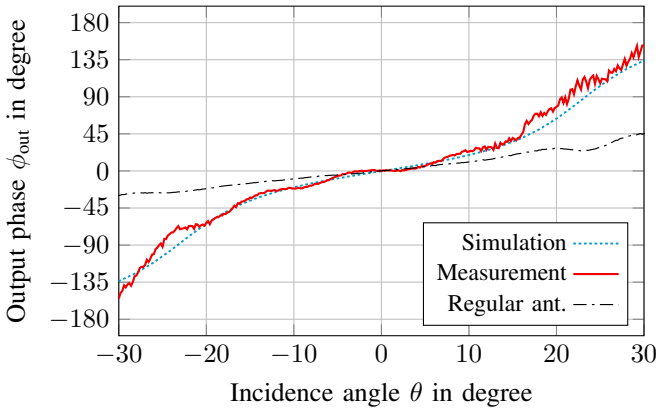

(a) Simulated and measured phase difference ϕ_{out} at the output of the BMAA at 20.1 GHz. For comparison, the measured phase progression of the conventional antenna array (i.e. ϕ_{in}) is also given.

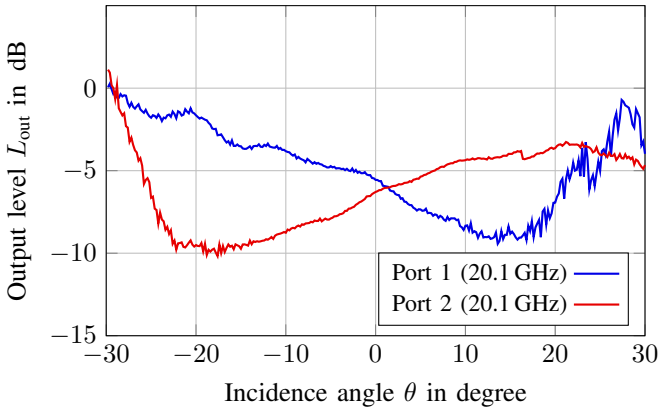

(b) Measured output power level L_{out} of the BMAA at 20.1 GHz for port 1 and port 2.

Fig. 4. Measured output phase progression (a) and output power level L_{out} (b) of the BMAA at 20.1 GHz.

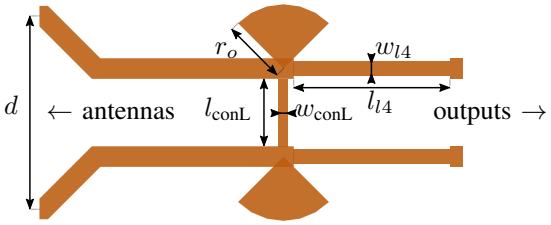

Fig. 5. Layout of the coupling network of the designed BMAA.

Table 1. Dimensions of coupling network of the fabricated BMAA.

w_{conL}	l_{conL}	w_{l4}	l_{l4}	r_o
0.15 mm	1.05 mm	0.22 mm	2.43 mm	1 mm

The value for ξ_{ob} was hereby calculated using (5) and the following abbreviations were used:

$$G = G_L + G_{11}, \tag{9}$$

$$a = B_{11} - B_{12} + B_1 + B_2, \tag{10}$$

$$b = B_{11} + B_{12} + B_1, \tag{11}$$

with $Y_{11} = G_{11} + \mathrm{j}B_{11}$ and $Y_{12} = G_{12} + \mathrm{j}B_{12}$ being the Y-Parameters of the antenna. The respective length of the microstrip line segments were then calculated from the lumped element values and optimized by full wave simulations. The final dimensions of the fabricated coupling network are listed in Tab. 1.

The fabricated BMAA was measured in an anechoic chamber using a four-port VNA to get the phase difference curves. For the calculation of the output power level L_{out}, a similar antenna without coupling network was also measured with the same setup. Both results, phase difference and output power level, are depicted in Fig. 4.

The measured phase difference ϕ_{out} in Fig. 4(a) matches well with the simulated values. The measured phase gain η_{ob} at $\pm 20°$ is approx. 12 and in very good agreement with the simulation results. For comparison, the phase difference curve of the conventional antenna array is also plotted and follows the theoretical course of $kd \sin\theta$.

Figure 4(b) shows the output power level L_{out} normalized to the uncoupled conventional antenna. It shows a power level of -6 dB in boresight direction as well as -10 dB and -8 dB for $\theta = -20°$ and $\theta = 20°$, respectively.

Despite the high values of L_{out}, the quality criterion at 20° is still fulfilled

$$\eta_{\text{ob}} \sqrt{L_{\text{out}}} = 12 \sqrt{10^{-10\,\text{dB}\,/10}} = 3.8\ , \tag{12}$$

clearly indicating the advantages of this BMAA.

V. Radar Measurements

To verify the enhanced angle estimation capabilities, radar measurements were taken in an anechoic chamber. A bistatic radar was set-up on a turntable with a K-band horn antenna as transmitting antenna and the BMAA as receiving antenna array. A corner reflector with an RCS of 2.7 dBsm was placed at a distance of 2 m in front of the radar. The measurement setup is depicted in Fig. 6.

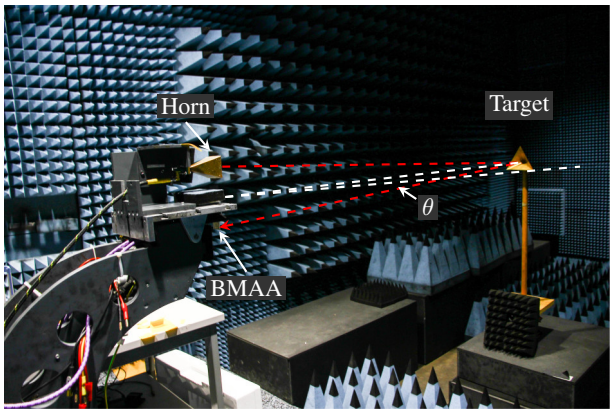

Fig. 6. Photograph of the measurement setup in the anechoic chamber.

To perform Maximum Likelihood (ML) angle estimation, a calibration dataset had to be recorded first. It was taken by

rotating the radar in the angular range from $-40°$ to $40°$ with the corner reflector placed at $\theta = 0°$. Then, the target was placed under different angles θ_0 with respect to the radar and 100 measurements were performed for each angle to see the variations between each measurement. For comparison, the same measurements were taken with a conventional antenna which is absolutely identical to the BMAA except for the biomimetic coupling network.

The measurement results are plotted in Fig. 7. Fig. 7(a)

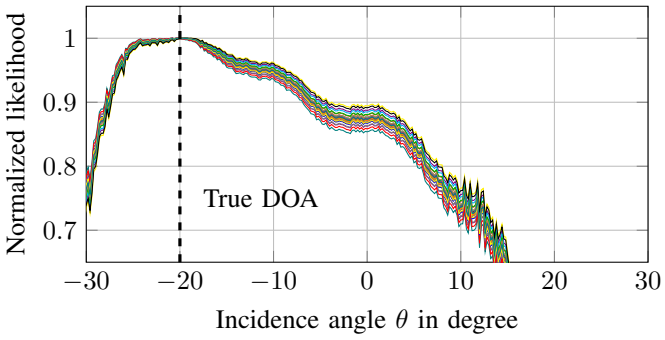

(a) BMAA at 20.1 GHz.

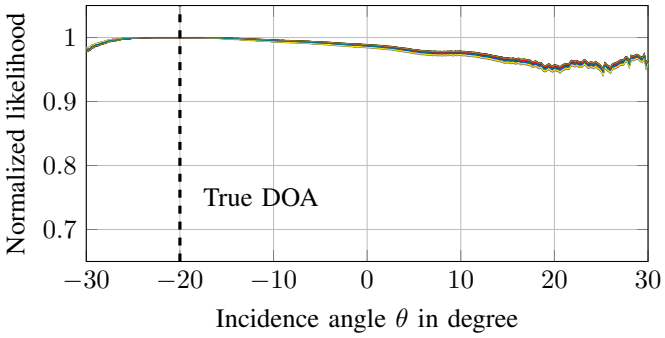

(b) Regular antenna array at 20.1 GHz.

Fig. 7. Normalized likelihood functions of 30 out of 100 measurements for a radar using the BMAA (a) and the conventional antenna (b) with a target placed at $\theta = -20°$.

shows the normalized likelihood plots for a target placed at an angle of $-20°$ while Fig. 7(b) shows the same plot for the conventional antenna. As can be seen, the likelihood function of the BMAA has a much smaller lobe compared to the conventional antenna due to the significantly increased off-boresight phase enhancement factor η_{ob}. The narrower lobe enables a much more precise angle estimation especially with very noisy signals. On the other hand, the likelihood plot is apparently more sensitive to noise due to the decrease in output power according to L_{out}.

In a next step, the maxima of the likelihood functions were extracted for each of the measurements. Figure 8 shows the distribution of the angle estimation error $\Delta\theta$, which is defined as the difference of measured angle θ_{m} and actual angle θ_0 of the target. It can be seen that the distribution of the angle estimation error of the BMAA has much less variance around the true value with a standard deviation of $0.38°$. In contrast, the angle estimation error of the conventional antenna

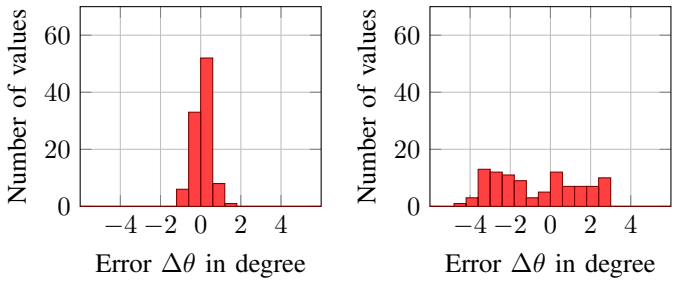

(a) BMAA at 20.1 GHz (b) Conv. antenna at 20.1 GHz

Fig. 8. Distribution of angle estimation errors out of 100 measurements for a target placed at $-20°$.

array shows a much higher variance with a standard deviation of $2.10°$.

VI. Conclusion

In this paper, a biomimetic antenna array was shown which is able to enhance the angle estimation for off-boresight targets. A generalized phase enhancement factor η_{ob} was derived and a prototype for $\theta_{\text{ob}} = 20°$ was fabricated and measured. Radar measurements show a significant increase in angle estimation capability. All investigations are hereby based on the current BMAA theory so that only the element values of the coupling network need to be changed. However, in future work it may be applicable that an electronically tunable coupling network, e.g. like it is shown in [7], is implemented to allow for a dynamically changing ϕ_{out} curve.

Acknowledgement

This work was funded by the German Research Foundation (DFG, Deutsche Forschungsgemeinschaft) – WA 3506/6-1.

References

[1] R. N. Miles, D. Robert, and R. R. Hoy, "Mechanically coupled ears for directional hearing in the parasitoid fly Ormia ochracea," *The Journal of the Acoustical Society of America*, vol. 98, no. 6, Dec. 1995.

[2] A. Masoumi, Y. Yusuf, and N. Behdad, "Biomimetic Antenna Arrays Based on the Directional Hearing Mechanism of the Parasitoid Fly Ormia Ochracea," *IEEE Transactions on Antennas and Propagation*, vol. 61, no. 5, pp. 2500–2510, May 2013.

[3] P. Grüner, T. Chaloun, and C. Waldschmidt, "Towards a mm-Wave Planar Biomimetic Antenna Array with Enhanced Phase Sensitivity," in *10th European Conference on Antennas and Propagation (EuCAP)*, Davos, 2016.

[4] J. Zhong, A. Kiourti, and J. Volakis, "Reducing and Controlling the Beamwidth of Electrically Small Antenna Arrays," in *9th European Conference on Antennas and Propagation (EuCAP)*, Apr. 2015, pp. 1–2.

[5] A. Masoumi and N. Behdad, "An Improved Architecture for Two-Element Biomimetic Antenna Arrays," *IEEE Transactions on Antennas and Propagation*, vol. 61, no. 12, pp. 6224–6228, Dec. 2013.

[6] P. Grüner, T. Chaloun, and C. Waldschmidt, "Enhanced Angle Estimation Accuracy of Ultra Compact Radars Inspired by a Biomimetic Approach," in *IEEE MTT-S International Microwave Symposium (IMS)*, Honolulu, HI, Jun. 2017.

[7] M. R. Nikkhah, K. Ghaemi, and N. Behdad, "An Electronically Tunable Biomimetic Antenna Array," *IEEE Transactions on Antennas and Propagation*, vol. PP, no. 99, pp. 1–1, 2018.